



## Functionalized nano magnetic Fe<sub>3</sub>O<sub>4</sub>-SiO<sub>2</sub> core-shell as efficient adsorbent for removal of Pb<sup>2+</sup> from aqueous solutions

A. Mokhtari Baghkumeh, H. Faghihian\*, Sh. Mokhtari

Department of Chemistry, Shahreza Branch, Islamic Azad University, P.O. Box 311-86145, Shahreza, Isfahan, Iran, Tel. +98 321-3292515; Fax: +98 321-3291018; emails: faghihian@iaush.ac.ir (H. Faghihian), mokhtariali99@yahoo.com (A.M. Baghkumeh), sheida\_m20062006@yahoo.com (S. Mokhtari)

Received 22 April 2016; Accepted 10 December 2016

### ABSTRACT

Development of reliable adsorbents with high adsorption capacity, fast adsorption-desorption kinetics is of significant importance. Nanosized magnetic particles having high surface area and unique advantage of easy separation by external magnetic field are considered as potential adsorbents for removal of heavy metal cations from aqueous solutions. In this research, synthesis of Fe<sub>3</sub>O<sub>4</sub>-SiO<sub>2</sub> core-shell and its efficiency for removal of Pb<sup>2+</sup> from aqueous solution has been reported. In order to increase the adsorption capacity, the magnetic adsorbent was modified with 2-aminothiophenol. The modified adsorbent was characterized by Fourier transform infrared spectroscopy, scanning electron microscopy, Brunauer-Emmett-Teller and thermogravimetry techniques. At optimized conditions, the adsorbent capacity of 60 mg g<sup>-1</sup> was obtained. The adsorption process was kinetically fast, and more than 60% of the adsorption capacity was obtained within 10 min. The magnetic nanoparticles carrying the target cation were easily separated from the solution by applying an external magnetic field. Regeneration of the used adsorbent showed that its capacity slightly declined with the number of regeneration. However, 83.71% of initial adsorption capacity was remained after four-step regeneration cycle.

*Keywords:* Core-shell; Magnetic nanomaterial; SiO<sub>2</sub>; Functionalization; Adsorption; Pb<sup>2+</sup>

### 1. Introduction

Lead is one of the basic heavy elements, which can be combined with other substances to form lead compounds in a variety of products, including gasoline, paint, storage batteries, plumbing, fine crystal, electric cable insulation, ammunition and insecticides. Lead poisoning is the leading environmental health risk, particularly in young children. Lead has the ability to impede the development and function of every organ and system in the body. Once it enters the body, lead travels through the blood stream, and most of it are stored in the bones, and some are deposited in the kidneys and brain. Lead stays in the body for a long time. The "half life" of lead in bone can be more than 20 years. Health impact of lead exposure includes; various forms of blood disorders and anemia, rapid deterioration of brain and the

nervous system, reduced fertility both in men and women, failure of the kidney, and Alzheimer's disease [1]. The allowable level of lead in drinking water has been reduced from 0.6 to 0.05 ppm. However, no level of lead is considered actually safe today. Consequently, elimination of lead is an essential way for purification of aqueous wastes to meet the increasingly stringent environmental requirements [2]. Removal of lead from water and liquid wastes has been conducted by several methods including precipitation, ion exchange and adsorption. Among them, adsorption method has been found to be superior to other techniques for effective lead removal in term of cost, simplicity of design and ease of operation [3,4]. As an adsorbent, silica is an inexpensive abundant material, inert to redox reactions, stable in acidic solutions with high mass exchange and thermal resistance.

Nanosized materials due to large surface area and highly active surface have a wide range of potential applications as adsorbents [5]. The major drawback of nanoparticles applied

\* Corresponding author.

as adsorbent is the tedious filtration or centrifugation steps need to separate and recover the nanoparticles from the reaction solution. Therefore, many approaches were established to solve these issues by utilization of core-shell adsorbent in which the magnetic materials is the core of adsorbent and  $\text{SiO}_2$  as an ideal shell to protect the inner magnetite cores [6–12]. To promote the adsorption capacity and selectivity of nanomaterials, surface modification has often been explored to enable specific metal complex formation [13,14]. For removal of a wide variety of heavy metal ions, functionalized materials demonstrated outstanding ability [15–19].

In this paper, magnetic  $\text{Fe}_3\text{O}_4$ - $\text{SiO}_2$  core-shell ( $\text{Fe}_3\text{O}_4$ - $\text{SiO}_2$ -CS) was first prepared and then functionalized with 2-aminothiophenol. The functionalized adsorbent was employed for adsorption of lead from aqueous solution under different experimental conditions.

## 2. Materials and methods

$\text{FeCl}_3 \cdot 6\text{H}_2\text{O}$ ,  $\text{FeCl}_2 \cdot 4\text{H}_2\text{O}$ , 2-aminothiophenol, sodium silicate, sodium hydroxide, hydrochloric acid, nitric acid and ethanol were purchased from Merck Company (Germany). Deionized water was used throughout the experiments. Lead Concentration was measured by flame atomic absorption spectrometry by using AAnalyst 300 instrument (USA). The pH of the solutions was measured by a Denver, UltraBasic, UB-10 digital pH meter (USA). Infrared spectra were recorded on a Perkin Elmer 65 FT-IR apparatus (USA). The scanning electron microscopy (SEM) and transmission electron microscopy (TEM) images were prepared by Zeiss Ultra 55 instrument. The thermogravimetry–differential thermal gravimetry (TG–DTG) curves prepared by NETZSCH STA 409 PC/PG instrument from room temperature to  $600^\circ\text{C}$  with heating rate of  $10^\circ\text{C min}^{-1}$ .

### 2.1. Preparation of magnetite nanoparticles

The magnetite nanoparticles were prepared by the conventional co-precipitation method. Briefly, 0.04 mol of  $\text{FeCl}_3 \cdot 6\text{H}_2\text{O}$  and 0.02 mol of  $\text{FeCl}_2 \cdot 4\text{H}_2\text{O}$  were dissolved in 50 mL of 0.5 M HCl solution. The solution was then added dropwise to 500 mL of  $1.5 \text{ mol L}^{-1}$  of sodium hydroxide solution at  $80^\circ\text{C}$  under nitrogen flow with vigorous stirring. The obtained  $\text{Fe}_3\text{O}_4$  nanoparticles were repeatedly washed with deionized water followed by drying at  $50^\circ\text{C}$  under vacuum for 4 h.

### 2.2. Preparation and functionalization of $\text{Fe}_3\text{O}_4$ - $\text{SiO}_2$ core-shell

To prepare silica-coated  $\text{Fe}_3\text{O}_4$  nanoparticles, 2 g of  $\text{Fe}_3\text{O}_4$  nanoparticles were suspended in 400 mL deionized water, heated to  $80^\circ\text{C}$  under nitrogen flow. Forty milliliters of 1.0 M sodium silicate solution was then added dropwise to the  $\text{Fe}_3\text{O}_4$  suspension under vigorous stirring for 2 h, and the pH of the mixture was adjusted to 6.0 with 2 M HCl solution. The mixture was further stirred at  $80^\circ\text{C}$  for 3 h. The resulting silica-coated  $\text{Fe}_3\text{O}_4$  nanoparticles were thoroughly washed with deionized water and collected by magnetic separation, followed by drying at  $50^\circ\text{C}$  under vacuum for 12 h. The materials obtained are referred to as  $\text{Fe}_3\text{O}_4$ - $\text{SiO}_2$ -CS. To prepare functionalized adsorbent, the silica-coated magnetite nanoparticles (2 g) were suspended in ethanol (100 mL) and then 2 mL of

2-aminothiophenol was added under dry nitrogen atmosphere. The mixture was refluxed for 12 h, and the solid was magnetically separated, washed with ethanol several times to remove the unreacted residues and then was vacuum dried at  $80^\circ\text{C}$ . The adsorbent was designated as Func- $\text{Fe}_3\text{O}_4$ - $\text{SiO}_2$ -CS. The synthetic route of Func- $\text{Fe}_3\text{O}_4$ - $\text{SiO}_2$ -CS is illustrated in Fig. 1.

### 2.3. Adsorption experiments

Stock solution of  $\text{Pb}^{2+}$  was prepared by dissolving appropriate amount of  $\text{Pb}(\text{NO}_3)_2$  in deionized water. The standard solutions of lead containing ( $6\text{--}30 \text{ mg L}^{-1}$ ) were prepared by the stock solution. Adsorption experiments were conducted by shaking of 0.1 g of the adsorbent with 25 mL of  $\text{Pb}^{2+}$  solution for known period. After equilibration, the adsorbent was separated by applying external magnetic field. The concentration of  $\text{Pb}^{2+}$  in the solution was measured by flame atomic absorption spectrometry. The effect of different parameters on the adsorption capacity was then evaluated.

## 3. Results and discussion

### 3.1. Characterization of the samples

The Fourier transform infrared spectroscopy (FTIR) spectra of the  $\text{Fe}_3\text{O}_4$  nanoparticles,  $\text{Fe}_3\text{O}_4$ - $\text{SiO}_2$ -CS, and Func- $\text{Fe}_3\text{O}_4$ - $\text{SiO}_2$ -CS are shown in Fig. 2. In the spectrum of

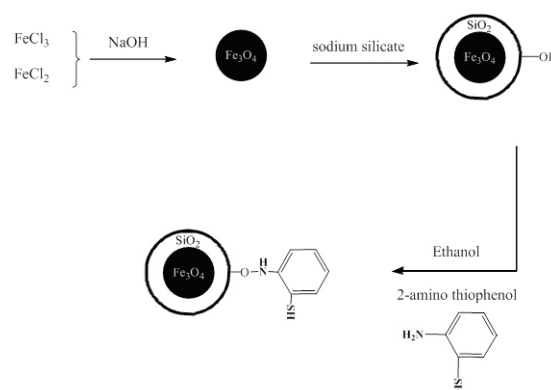


Fig. 1. Synthetic route of Func- $\text{Fe}_3\text{O}_4$ - $\text{SiO}_2$ -CS preparation.

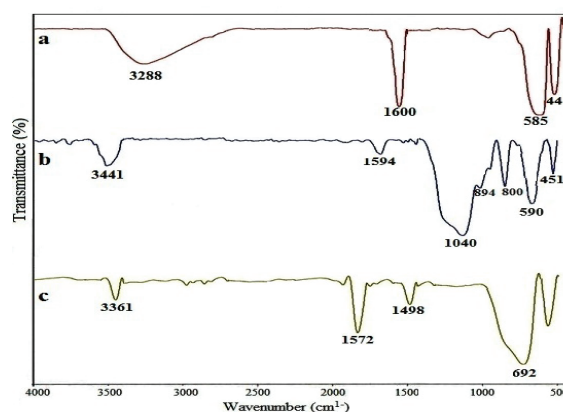


Fig. 2. FTIR spectra of: (a)  $\text{Fe}_3\text{O}_4$ , (b)  $\text{Fe}_3\text{O}_4$ - $\text{SiO}_2$ -CS, and (c) Func- $\text{Fe}_3\text{O}_4$ - $\text{SiO}_2$ -CS.

$\text{Fe}_3\text{O}_4$ , the absorption bands appeared at 3,288 and 1,600  $\text{cm}^{-1}$  were, respectively, attributed to the stretching and bending vibrations of O–H of water molecules, and the absorption peaks at 588 and 441  $\text{cm}^{-1}$  belonged to the stretching vibrations of Fe–O (Fig. 2(a)). In the spectrum of  $\text{Fe}_3\text{O}_4$ - $\text{SiO}_2$ -CS, besides the absorption bands of  $\text{Fe}_3\text{O}_4$  the absorption band of silica were also clearly observed. The band appeared at 3,441  $\text{cm}^{-1}$  was attributed to the stretching vibrations of Si–O–H, while the absorption bands related to the O–H was appeared at 1,594  $\text{cm}^{-1}$ . The bands at 1,040 and 800  $\text{cm}^{-1}$  were attributed to the stretching and bending vibrations of Si–O–Si, respectively. The absorption band related to the Si–O–Fe was appeared at 894  $\text{cm}^{-1}$  that reflected that the magnetite surface was coated by silica (Fig. 2(b)). The vibration bond appeared at 3,361, 1,572, 1,498 and 692  $\text{cm}^{-1}$  of the Func- $\text{Fe}_3\text{O}_4$ - $\text{SiO}_2$ -CS sample was related to the presence of amino groups and indicating that 2-aminothiophenol functional group has been grafted on the surface of the magnetic core-shell (Fig. 2(c)).

The SEM images of  $\text{Fe}_3\text{O}_4$ ,  $\text{Fe}_3\text{O}_4$ - $\text{SiO}_2$ -CS and Func- $\text{Fe}_3\text{O}_4$ - $\text{SiO}_2$ -CS samples were used to figure out the changes occurred on the surface morphology of the sample after each treatment. In the SEM image of magnetite nanoparticles, relatively high condensed spherical particles were observed. The average size of the particle was estimated to be 60 nm (Fig. 3(a)). In the SEM image of the  $\text{Fe}_3\text{O}_4$ - $\text{SiO}_2$ -CS, it was clearly observed that the surface of  $\text{Fe}_3\text{O}_4$  has been coated by silica (Fig. 3(b)). In the TEM of this sample, a shadow-like shell was formed around the dense magnetic core (Fig. 2(c)). In the SEM image of Func- $\text{Fe}_3\text{O}_4$ - $\text{SiO}_2$ -CS, the nanoparticles covered by the grafted amine were appeared as cloudy aggregated particles (Fig. 3(c)).

Fig. 4 shows the magnetic hysteresis loop of  $\text{Fe}_3\text{O}_4$ - $\text{SiO}_2$ -CS, and Func- $\text{Fe}_3\text{O}_4$ - $\text{SiO}_2$ -CS nanocomposites. The saturation magnetization of  $\text{Fe}_3\text{O}_4$ - $\text{SiO}_2$ -CS and Func- $\text{Fe}_3\text{O}_4$ - $\text{SiO}_2$ -CS was measured, respectively, as 42.68 and 38.46  $\text{emu g}^{-1}$ . Both samples exhibited superparamagnetic behavior at room temperature with no coercivity and remanence. It can be seen that the saturation magnetization value was decreased after modification of the core-shell by 2-aminothiophenol. This can be attributed to the formation of a nonmagnetic layer of the ligand on the surface of the adsorbent. However, the superparamagnetic behavior of the samples at room temperature indicated that they can be separated from aqueous solution by magnetic separation technique (Fig. 4).

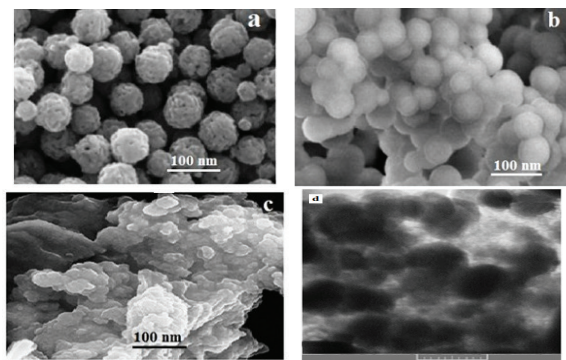


Fig. 3. SEM images of: (a)  $\text{Fe}_3\text{O}_4$ , (b)  $\text{Fe}_3\text{O}_4$ - $\text{SiO}_2$ -CS, (c) Func- $\text{Fe}_3\text{O}_4$ - $\text{SiO}_2$ -CS and (d) TEM image of  $\text{Fe}_3\text{O}_4$ - $\text{SiO}_2$ -CS.

In the thermal curve (TG and DTG) of  $\text{Fe}_3\text{O}_4$ - $\text{SiO}_2$ -CS sample, two separate weight loss peaks was distinguished. The first small weight loss appeared below 150°C was attributed to the evaporation of water molecules from the surface of the silica layer. Another weight loss above 500°C was associated with the release of the structure water (Fig. 5(a)). The thermal curve of Func- $\text{Fe}_3\text{O}_4$ - $\text{SiO}_2$ -CS showed a gradual weight loss between 200°C and 300°C, which was attributed to the water desorption of the sample. The second weight loss started from 200°C and ended at 600°C was resulted from the decomposition of aminothiophenol groups grafted to the silica surface (Fig. 5(b)) [20].

The Brunauer–Emmett–Teller surface area and pore volume of  $\text{Fe}_3\text{O}_4$ / $\text{SiO}_2$  core-shell was, respectively, 348  $\text{m}^2 \text{g}^{-1}$  and 0.34  $\text{cm}^3 \text{g}^{-1}$  and close to the previous reported values [21]. For the functionalized  $\text{Fe}_3\text{O}_4$ / $\text{SiO}_2$  the surface area and pore volume were, respectively, to 327  $\text{m}^2 \text{g}^{-1}$  and 0.29  $\text{cm}^3 \text{g}^{-1}$ . The small reduction can be attributed to the coverage of the surface by 2-aminothiophenol.

### 3.2. Adsorption experiments

#### 3.2.1. Effect of initial concentration

To determine the quantity of the adsorbent needed for removal of specific amount of metal ions from aqueous

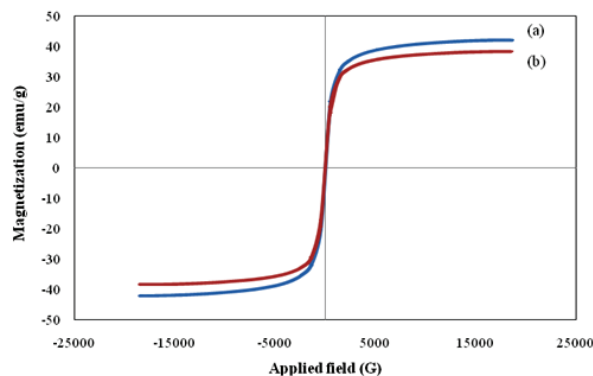


Fig. 4. Magnetization curve of: (a)  $\text{Fe}_3\text{O}_4$ - $\text{SiO}_2$ -CS and (b) Func- $\text{Fe}_3\text{O}_4$ - $\text{SiO}_2$ -CS.

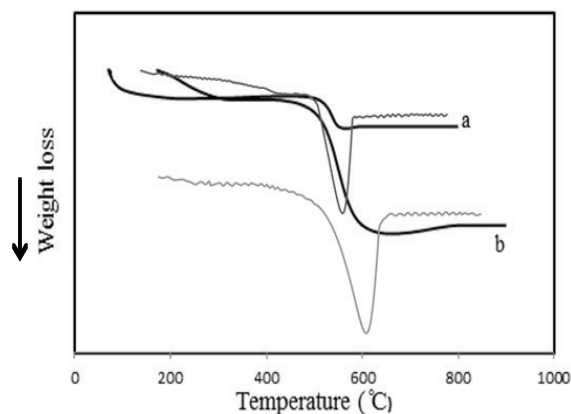


Fig. 5. Thermal curves (TG and DTG) of: (a)  $\text{Fe}_3\text{O}_4$ - $\text{SiO}_2$ -CS and (b) Func- $\text{Fe}_3\text{O}_4$ - $\text{SiO}_2$ -CS.

solution, the adsorption capacity of the adsorbent must be determined. To measure the adsorption capacity, 10 mL of  $Pb^{2+}$  solution (between 50 and 1,000 mg L<sup>-1</sup>) was put in contact with 0.1 g of the adsorbent at pH = 4, and the mixture was shaken for 120 min. The adsorbent was separated, and the  $Pb^{2+}$  concentration in the solution was measured. The results indicated that the adsorption capacity was increased with the increase of initial  $Pb^{2+}$  concentration until the equilibrium was established (Fig. 6). The adsorption capacity of Func- $Fe_3O_4$ - $SiO_2$ -CS was almost twice of the value obtained for  $Fe_3O_4$ - $SiO_2$ -CS indicating the importance of functionalization of the core-shell adsorbent. Different adsorbents have been used for removal of heavy metal from aqueous solutions. Wang et al. [22] used modified- $Fe_3O_4/SiO_2$  for removal of  $Cu^{2+}$ ,  $Pb^{2+}$  and  $Cd^{2+}$ , and reported the adsorption capacity of 30.8, 76.6 and 22.4 mg g<sup>-1</sup> for the studied ions, respectively [22]. Ge [23] used polymer-modified magnetic nanoparticles for removal of  $Cd^{2+}$ ,  $Zn^{2+}$ ,  $Pb^{2+}$  and  $Cu^{2+}$ , and reported the optimal adsorption capacity of 29.6, 166.1, 43.4 and 126.9 mg g<sup>-1</sup>, respectively [23]. The adsorption capacity of the modified adsorbent of this work was higher than the reported values for similar adsorbents.

### 3.2.2. Effect of pH

pH plays an important role in the adsorption process. The pH change can alter surface charge of the adsorbent, the abundant of different adsorbate species and the concentration of  $H_3O^+$  and  $OH^-$ . Based on the experimental results, it was concluded that by increasing pH, the adsorption capacity was enhanced and the maximal value was obtained at pH = 4 (Fig. 7). This observation is consistent with the metal-amine complexation mechanism, as the amino groups are protonized at low pH, passivating adsorption sites and hence suppressing metal adsorption. The dependence of adsorption capacity on pH may also be attributed to the change in the surface charge of the adsorbent, which was consistent with the pH-dependent zeta potential of the adsorbent. Moreover, at low pHs, the adsorption sites are protonated, and  $H_3O^+$  competes with  $Pb^{2+}$  for the adsorption sites [22]. At higher pHs, the electron pairs of nitrogen of the ligand interact with  $Pb^{2+}$  and increased the adsorption capacity. The optimized pH of each

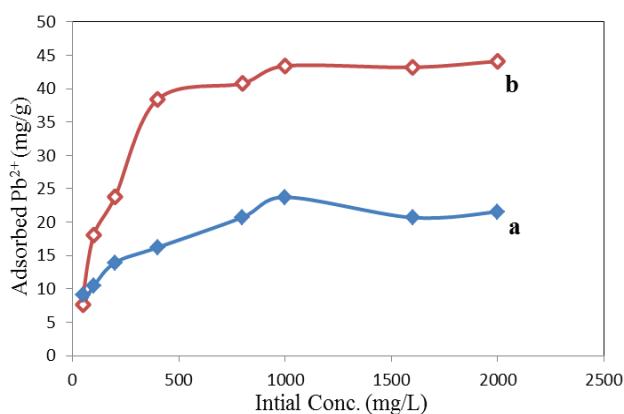


Fig. 6. Effect of Initial concentrations on the adsorption capacity (adsorbent dose = 0.1 g, shaking time = 2 h, pH = 4, Temp = 25°C): (a)  $Fe_3O_4$ - $SiO_2$ -CS and (b) Func- $Fe_3O_4$ - $SiO_2$ -CS.

adsorbent depends on its surface charge, and hence different adsorbents depending to their  $PH_{pzc}$  values have their appropriate optimized pH. For example, in the modified  $Fe_3O_4@SiO_2-NH_2^+$  adsorbent, the maximal adsorption capacity was achieved at pH = 6 [7] while in dithizone-modified  $Fe_3O_4@SiO_2$  and bismuthiol-II-immobilized magnetic nanoparticle adsorbents, the maximal adsorption capacity was achieved at pH = 7 [24–26].

### 3.2.3. Kinetics of adsorption process

Adsorption of  $Pb^{2+}$  was studied at different time intervals (2–180 min; Fig. 8). Although the equilibrium was established within 120 min, the metal adsorption in the early stages of the process was fast, and more than 60% of the adsorbent capacity was achieved within 20 min. It was suggested that adsorption process proceeded in two stages. The majority of the adsorption sites were engaged at first stage, and the remaining sites were occupied in a gradual and slower step until equilibration was established. Reaction kinetic is either reviewed by the first-order model, which assumes that the adsorption process is controlled by penetration, or by the second-order equation, which assumes that the adsorption process involved a chemical reaction [27,28]. According to the kinetic parameters

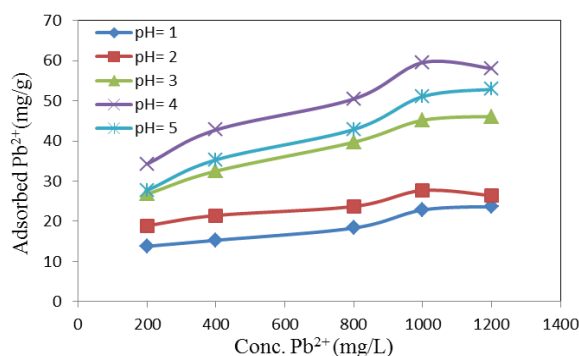


Fig. 7. Effect of pH on the adsorption of  $Pb^{2+}$  by Func- $Fe_3O_4$ - $SiO_2$ -CS (adsorbent dose = 0.1 g, shaking time = h, temp = 25°C).

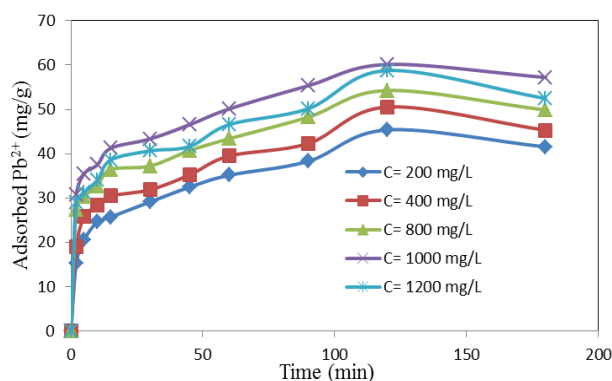


Fig. 8. Effect of time on  $Pb^{2+}$  adsorption by Func- $Fe_3O_4$ - $SiO_2$ -CS (adsorbent dose = 0.1 g, initial concentration = 200–1,200 mg L<sup>-1</sup>, pH = 4, Temp = 25°C).

calculated for pseudo-first-order and pseudo-second-order models (Table 1), it was concluded that the correlation coefficient values for pseudo-first order was lower than the values obtained for the second-order models indicating the chemical nature of the adsorption process. The equilibration time for nanoalumina used for adsorption of  $\text{Cd}^{2+}$  and  $\text{Pb}^{2+}$  was 120 min [25]. The chemical nature of the adsorption and the fast kinetic of the adsorption can be considered as the advantage of the method for removal of lead from aqueous solutions by continuous column operation.

### 3.2.4. Adsorption isotherms

The adsorption isotherms express the relationship between the amounts of adsorbed species onto the adsorbent and its concentration in solution at equilibrium. Several isotherm models including Langmuir and Freundlich have been proposed. The Langmuir and Freundlich models evaluated the adsorption experimental data, and the results are summarized in Table 2.

The correlation coefficient for Langmuir isotherm was 0.9988 and higher than the value obtained for Freundlich isotherm. The  $K_L$  value of 0.023 confirmed that adsorption process was optimal and non-linear. Among the studies in this field, we may mention the adsorption isotherms by magnetic nanoparticles used for lead removal that followed the Langmuir model [22].

### 3.2.5. Effect of temperature

The temperature plays an important role in the adsorption process. As shown in Fig. 9, the adsorption capacity of lead onto Func- $\text{Fe}_3\text{O}_4$ - $\text{SiO}_2$ -CS increased as the solution temperature increased from 25°C to 55°C. The increase in the adsorption capacity with the increase of temperature was attributed to endothermic nature of the process. At higher temperature, the required energy for the reaction progress was supplied, and the diffusion of lead to the adsorption site was facilitated. In a research conducted by Mokhtari and Faghihian [24], functionalized activated carbon was used for separation of  $\text{Hg}^{2+}$  from aqueous solutions. They reported that the adsorption process was chemisorptions and exothermic.

Table 1  
Correlation coefficient values for kinetic models for  $\text{Pb}^{2+}$  adsorption

Kinetic models	$R^2$	$K$
Pseudo-first-order	0.9777	0.0186
Pseudo-second-order	0.9903	0.062

Table 2  
Langmuir and Freundlich isotherm parameters

Adsorbent	Adsorbed	Langmuir isotherm			Freundlich isotherm		
		$q_m$ ( $\text{mg g}^{-1}$ )	$K_L$ ( $\text{L mg}^{-1}$ )	$R^2$	$N$	$k_f$	$R^2$
Func- $\text{Fe}_3\text{O}_4$ - $\text{SiO}_2$ -CS	$\text{Pb}^{2+}$	44.84	0.023	0.9988	4.16	32.80	0.9213

### 3.3. Regeneration of the adsorbent

The regeneration of adsorbent, i.e., the restoration of adsorption capability, is a crucial factor in practical application of the adsorbent. Prior to evaluate the reusability of the adsorbent, its stability under acidic conditions was examined. 0.1 g of the adsorbent was dispersed in 50 mL of 1 M  $\text{HNO}_3$  solution. After continuous contact with acid for 24 h, the suspension was magnetically separated, and iron concentration in the supernatant was determined. The results showed that the iron concentration was insignificant indicating that the silica shell properly protected the magnetic core of the adsorbent against acidic conditions. The suppressed adsorption of lead observed on Func- $\text{Fe}_3\text{O}_4$ - $\text{SiO}_2$ -CS nanoparticles at low pH and high stability of the adsorbent under acidic conditions implied that acid treatment was a feasible approach to regenerating the loaded adsorbent. To regenerate the used adsorbent, it was eluted with 20 mL of 1.0 M  $\text{HNO}_3$  solution. In the second adsorption experiment with the regenerated adsorbent, the adsorption capacity of 97.56% was obtained. The decrease was attributed to the blockage of some adsorption sites, decomposition or separation of the ligand from the adsorbent surface (Fig. 10).

## 4. Conclusion

A nanosized magnetic core-shell was prepared and modified with 2-aminothiophenol. High adsorption capacity toward  $\text{Pb}^{2+}$  was achieved through complexation of metal ions by the ligand grafted on the silica surface of the adsorbent. The modified adsorbent was highly monodisperse and magnetically separable. The core-shell structure of the nanoadsorbent formed by a magnetite wrapped with an inert silica layer provided ease of magnetic separation and protection from acid leaching in regeneration. The adsorbent was

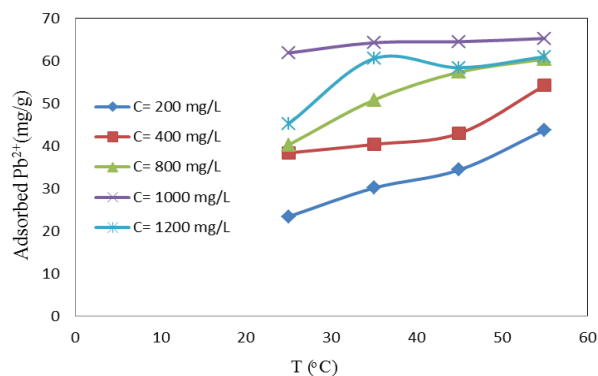


Fig. 9. Effect of temperature on  $\text{Pb}^{2+}$  adsorption onto Func- $\text{Fe}_3\text{O}_4$ - $\text{SiO}_2$ -CS (adsorbent dose = 0.1 g, initial concentration = 200–1,200  $\text{mg L}^{-1}$ , pH = 4, shaking time = 120 min).

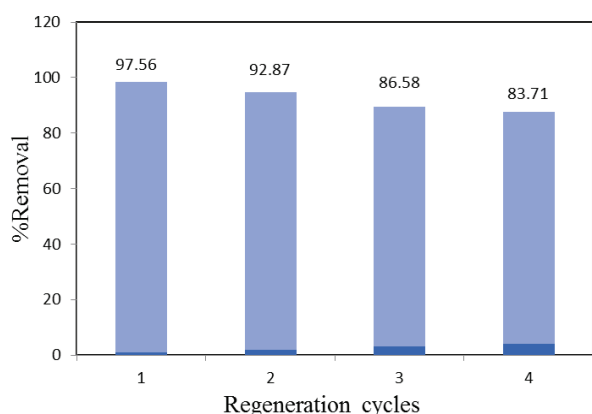


Fig. 10. Reusability of Func-Fe<sub>3</sub>O<sub>4</sub>-SiO<sub>2</sub>-CS for Pb<sup>2+</sup> removal.

characterized by FTIR, SEM, vibrating sample magnetometry and TG-DTG techniques. The adsorption process was kinetically fast, and more than 60% of the adsorption capacity was obtained within 20 min. With these unique features, the Func-Fe<sub>3</sub>O<sub>4</sub>-SiO<sub>2</sub>-CS nanoparticles showed a high potential for effective removal of lead in water treatment.

## References

- [1] R.M. Brooks, M. Bahadory, F. Tovia, H. Rostami, Removal of lead from contaminated water, *Int. J. Soil Sediment Water*, 3 (2010) 1–14.
- [2] G. Cheng, M. He, H. Peng, B. Hu, Dithizone modified magnetic nanoparticles for fast and selective solid phase extraction of trace elements in environmental and biological samples prior to their determination by ICP-OES, *Talanta*, 88 (2012) 507–515.
- [3] W. Yantasee, C.L. Warner, T. Sangvanich, R.S. Addleman, T.G. Carter, R.J. Wiacek, G.E. Fryxell, C. Timchalk, M.G. Warner, Removal of heavy metals from aqueous systems with thiol functionalized superparamagnetic nanoparticles, *Environ. Sci. Technol.*, 41 (2007) 5114–5119.
- [4] J.F. Liu, Z.S. Zhao, G.B. Jiang, Coating Fe<sub>3</sub>O<sub>4</sub> magnetic nanoparticles with humic acid for high efficient removal of heavy metals in water, *Environ. Sci. Technol.*, 42 (2008) 6949–6954.
- [5] Y.T. Zhou, H.L. Nie, C. Branford-White, Z.Y. He, L.M. Zhu, Removal of Cu<sup>2+</sup> from aqueous solution by chitosan-coated magnetic nanoparticles modified with  $\alpha$ -ketoglutaric acid, *J. Colloid Interface Sci.*, 330 (2009) 29–37.
- [6] L.J. Zhang, X.J. Chang, Y.H. Zhai, Q. Huang, Z. Hu, N. Jiang, Selective solid phase extraction of trace Sc(III) from environmental samples using silica gel modified with 4-(2-morinyldiazenyl)-N-(3-(trimethylsilyl)propyl) benzamide, *Anal. Chim. Acta*, 629 (2008) 84–91.
- [7] Z. Xu, Y. Feng, X. Liu, M. Guan, C. Zhao, H. Zhang, Synthesis and characterization of Fe<sub>3</sub>O<sub>4</sub>@SiO<sub>2</sub>@poly-L-alanine, peptide brush-magnetic microspheres through NCA chemistry for drug delivery and enrichment of BSA, *Colloids Surf., B*, 81 (2010) 503–507.
- [8] Z. Xu, B. Feng, S. Bian, T. Liu, M. Wang, Y. Gao, D. Sun, X. Gao, Monodisperse and core-shell structured SiO<sub>2</sub>@Lu<sub>2</sub>O<sub>3</sub>:Ln<sup>3+</sup> (Ln=Eu, Tb, Dy, Sm, Er, Ho, and Tm) spherical particles: a facile synthesis and luminescent properties, *J. Solid State Chem.*, 196 (2012) 301–308.
- [9] L. Wang, Y. Sun, J. Wang, J. Wang, A. Yu, H. Zhang, D. Song, Preparation of surface plasmon resonance biosensor based on magnetic core/shell Fe<sub>3</sub>O<sub>4</sub>/SiO<sub>2</sub> and Fe<sub>3</sub>O<sub>4</sub>/Ag/SiO<sub>2</sub> nanoparticles, *Colloids Surf., B*, 84 (2011) 190–484.
- [10] T. Peng, Y. Jiang, L. Xiao-Qin, Z. Dong-Yuan, S. Lin-Bing, Magnetically responsive core-shell Fe<sub>3</sub>O<sub>4</sub>@C adsorbent for efficient capture of aromatic sulfur and nitrogen compounds, *ACS Sustain. Chem. Eng.*, 4 (2016) 2223–2231.
- [11] J. Zhang, S. Zhai, S. Li, Z. Xiao, Y. Song, Q. An, G. Tian, Pb(II) removal of Fe<sub>3</sub>O<sub>4</sub>@SiO<sub>2</sub>-NH<sub>2</sub> core-shell nanomaterials prepared via a controllable sol-gel process, *Chem. Eng. J.*, 215 (2013) 461–471.
- [12] Z. Jian-Ming, Z. Shang-Ru, Z. Bin, T. Ge, Crucial factors affecting the physicochemical properties of sol-gel produced Fe<sub>3</sub>O<sub>4</sub>@SiO<sub>2</sub>-NH<sub>2</sub> core-shell nanomaterials, *J. Sol-Gel Sci. Technol.*, 66 (2012) 347–357.
- [13] C. Sun, R. Qu, C. Ji, C. Wang, Y. Sun, Z. Yue, G. Cheng, Preparation and adsorption properties of crosslinked polystyrene-supported low-generation diethanolamine-typed dendrimer for metal ions, *Talanta*, 70 (2006) 14–19.
- [14] J. Li, X. Miao, Y. Hao, J. Zhao, X. Sun, L. Wang, Synthesis, amino-functionalization of mesoporous silica and its adsorption of Cr(VI), *J. Colloid Interface Sci.*, 318 (2008) 309–314.
- [15] D. Shao, K. Xu, X. Song, J. Hu, W. Yang, C. Wang, Effective adsorption and separation of lysozyme with PAA-modified Fe<sub>3</sub>O<sub>4</sub>@silica core/shell microspheres, *J. Colloid Interface Sci.*, 336 (2009) 526–532.
- [16] O. Hakami, Y. Zhang, C.J. Banks, Thiol-functionalized mesoporous silica-coated magnetite nanoparticles for high efficiency removal and recovery of Hg from water, *Water Res.*, 46 (2012) 3913–3922.
- [17] A.M.L. Marzo, J. Pons, A. Merkoçi, Extremely fast and high Pb<sup>2+</sup> removal capacity using a nanostructured hybrid material, *J. Mater. Chem. A*, 2 (2014) 8766–8772.
- [18] Y. Zhang, L. Yan, W. Xu, X. Guo, L. Cui, L. Gao, Q. Wei, B. Du, Adsorption of Pb(II) and Hg(II) from aqueous solution using magnetic CoFe<sub>2</sub>O<sub>4</sub>-reduced graphene oxide, *J. Mol. Liq.*, 191 (2014) 177–182.
- [19] L. Cui, X. Guo, Q. Wei, Y. Wang, L. Gao, L. Yan, T. Yan, B. Du, Removal of mercury and methylene blue from aqueous solution by xanthate functionalized magnetic graphene oxide: sorption kinetic and uptake mechanism, *J. Colloid Interface Sci.*, 439 (2015) 112–120.
- [20] C.Z. Huang, B. Hu, Silica-coated magnetic nanoparticles modified with  $\gamma$ -mercaptopropyltrimethoxysilane for fast and selective solid phase extraction of trace amounts of Cd, Cu, Hg, and Pb in environmental and biological samples prior to their determination by inductively coupled plasma mass spectrometry, *Spectrochim. Acta, Part B*, 63 (2008) 437–444.
- [21] D. Yonghui, Q. Dawei, D. Chunhui, Z. Xiangmin, Z. Dongyuan, Superparamagnetic high-magnetization microspheres with an Fe<sub>3</sub>O<sub>4</sub>@SiO<sub>2</sub> core and perpendicularly aligned mesoporous SiO<sub>2</sub> shell for removal of microcystins, *J. Am. Chem. Soc.*, 130 (2008) 28–29.
- [22] J. Wang, S. Zheng, Y. Shao, J. Liu, Z. Xu, D. Zhu, Amino-functionalized Fe<sub>3</sub>O<sub>4</sub>@SiO<sub>2</sub> core-shell magnetic nanomaterial as a novel adsorbent for aqueous heavy metals removal, *J. Colloid Interface Sci.*, 349 (2010) 293–299.
- [23] F. Ge, M.-M. Li, H. Ye, B.-X. Zhao, Effective removal of heavy metal ions Cd<sup>2+</sup>, Zn<sup>2+</sup>, Pb<sup>2+</sup>, Cu<sup>2+</sup> from aqueous solution by polymer-modified magnetic nanoparticles, *J. Hazard. Mater.*, 15 (2012) 366–372.
- [24] S. Mokhtari, H. Faghian, Modification of activated carbon by 2,6-diaminopyridine for separation of Hg<sup>2+</sup> from aqueous solutions, *J. Environ. Chem. Eng.*, 3 (2015) 1662–1668.
- [25] M. Ezoddin, F. Shemirani, Application of modified nano-alumina as a solid phase extraction sorbent for the preconcentration of Cd and Pb in water and herbal samples prior to flame atomic absorption spectrometry determination, *J. Hazard. Mater.*, 178 (2010) 900–905.
- [26] J.S. Suleiman, B. Hu, H. Peng, C. Huang, Separation/preconcentration of trace amounts of immobilized magnetic nanoparticles and their determination by ICP-OES, *Talanta*, 77 (2009) 1579–1583.
- [27] A. Gunay, E. Arslankaya, I. Tosun, Lead removal from aqueous solution by natural and pretreated clinoptilolite zeolite: adsorption equilibrium and kinetics, *J. Hazard. Mater.*, 146 (2007) 362–371.
- [28] M. Al-Harashsheh, R.A. Shawabkeh, A. Al-harashsheh, M.M. Batiha, Surface modification and characterization of Jordanian kaolinite: application for lead removal from aqueous solutions, *Appl. Surf. Sci.*, 255 (2009) 8098–8103.